Modelling of Space Vector Pulse - Width Modulation for Electric Vehicles Application

Valentin Totev [a)] and Vultchan Gueorgiev [b)]

Faculty of Electrical Engineering, Technical University of Sofia, Sofia, Bulgaria

[a)] Corresponding author: valentintotev@tu-sofia.bg
[b)] vulchy@tu-sofia.bg

Abstract. This paper presents a discussion about modelling of space vector pulse – width modulation for electric vehicle application. As it is most commonly considered that a pulse – width modulation is symmetrical about its center, the considered modulation is based on the reversing alternating sequence space vector pulse – width modulation. Reversing alternating sequence is characterized with applying both null vectors V_0 and V_7 alternately. The modelling of the problem is done in MATLAB/ Simulink environment. Model mainly consists of a three – phase power converter with MOSFET's, a permanent magnet synchronous motor as they are highly utilized in modern electric vehicles and subsystems for computing sectors and gate signals for the inverter. The approach incorporates computing of sectors, time periods T_1, T_2 and T_0 which constitute operation of switches for each sector, and modulation of gate signals. Obtained results are purely on simulation level and are utilized to show that the expected nature of electrical quantities in steady state and transients is achievable even with simpler models.

INTRODUCTION

A discussion about space vector pulse – width modulation (SVPWM) and its simulation modelling is presented in this paper. The purpose is considered for electric vehicle (EV) application. EV's are more and more widely topical as a mean of transport with reduced or even without emissions. Currently, most EV's are driven by a permanent magnet synchronous motor (PMSM). A PMSM mainly consists of a three – phase stator coil and a rotor with permanent magnets. Motors of such type are characterized with higher power density, lower values of losses, higher torque and better dissipation of heat in comparison to induction motors.

An EV's motor is fed by the on- board battery pack through a power converter. As of yet the battery pack is the most important and most expensive component in EV's drivetrain system. It is formed by connecting multiple lithium – ion (Li – ion) batteries in series and in parallel. Power converter is usually a three – phased one and operates as an inverter whenever an EV is on the road. Power converter can also be operated as a three – phase rectifier [1]. This operation is utilized when an EV is performing regenerative braking which allows for part of energy used in braking to be recuperated back in the battery.

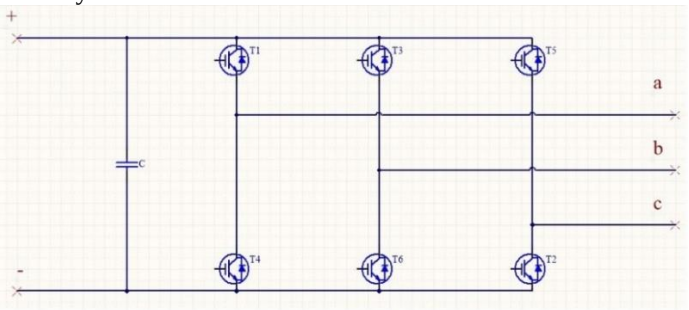

FIGURE 1. Three – phase inverter.

If a three – phase inverter with insulated gate bipolar transistors (IGBT) and flyback diodes, shown on Fig. 1, is considered and each of its transistors is considered as a switch, then each of inverter's legs can be in either of two states [2]. The first state is whenever the upper side IGBT is forward biased or in other words turned ON (closed switch) and lower side transistor is reverse biased or in other words turned OFF (open switch). The second state is the opposite as both transistors of the same inverter's leg cannot be ON at the same time (short circuit). Thus, points *a, b, c* on Fig. 1. can be considered as binary variables. Judging by the state of the upper side switch in each of inverter's legs, *a, b, c* can be equal to 1 whenever a respective leg is in first state and equal to 0 – for second state. This leads to $2^3 = 8$ possible combinations of states [2-9]. These eight switching combinations are further represented by Table 1. It can easily be found that inverter's output phase voltages can be determined by use of these binary variables as in (1) [2].

TABLE 1. Eight possible states of a three – phase inverter's legs.

State of a, b, c	Base voltage vector
[0 0 0]	V0
[0 0 1]	V1
[0 1 0]	V2
[0 1 1]	V3
[1 0 0]	V4
[1 0 1]	V5
[1 1 0]	V6
[1 1 1]	V7

$$\begin{bmatrix} V_{A0} \\ V_{B0} \\ V_{C0} \end{bmatrix} = \frac{1}{3} V_{dc} \begin{bmatrix} -2 & 1 & 1 \\ 1 & -2 & 1 \\ 1 & 1 & -2 \end{bmatrix} \begin{bmatrix} a \\ b \\ c \end{bmatrix} \quad (1)$$

where V_{A0}, V_{B0} and V_{C0} are inverter's output phase voltages and V_{dc} is DC bus voltage.

Usually, inverters are controlled by pulse – width modulation (PWM) where a given duty cycle ratio is considered. PWM in essence compares modulated signal (the three – phased sine waves) with a carrier one. Carrier signal is of triangular or sawtooth type and is with significantly higher frequency than modulated signal. In essence PWM produces gate signals according to the following operation. Whenever modulated sine waves have higher amplitudes than sawtooth wave, then upper side IGBT's are conducting. Analogously, whenever sine waves have lower amplitudes, then lower side IGBT's are ON [2]. Thus, by applying different duty cycles to the inverter, voltages with different magnitudes are obtained. Furthermore, depending on applied control algorithm (six – step commutation, sinusoidal PWM, SVPWM) inverter's output voltage has different utilization of DC bus voltage as shown by the space vector loci on Fig. 2 [2]. Six – step commutation is characterized with maximum utilization of DC voltage and output phase voltages have rectangular waveforms [2]. The spatial hexagon is described by six – step commutation, while the two types of PWM's describe circles.

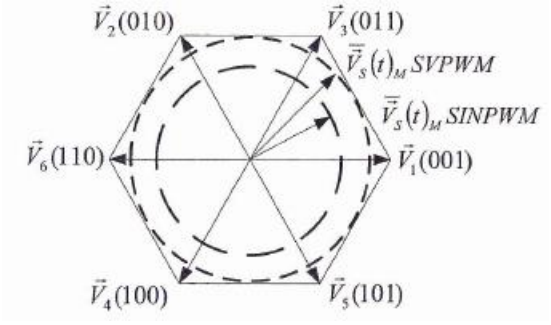

FIGURE 2. Space vector loci for different control algorithms [2].

SPACE VECTOR PULSE – WIDTH MODULATION

Proper control of an electric motor in order to achieve optimal drive of a process is necessary in every production process with electrical drives and EV's are no exception. An optimal regime is usually achieved whenever motor's torque and load's resistance torque are in a stable working point. Since the control of a separately excited DC motor is considered as the easiest, most accessible and most comfortable, control of other types of electric motors, even AC motors, is strived to be done in a similar conditions and similar manner. Thus, widely applied are Clarke's and Park's transformations. By performing these transformations respectively three – phase electrical quantities (currents or voltages) which are on a stationary reference frame can be transformed to two – phase quantities on a rotating reference frame [10-12]. The two transformations are given by (2) and (3) respectively.

$$\begin{bmatrix} v_\alpha \\ v_\beta \end{bmatrix} = \frac{2}{3}\begin{bmatrix} 1 & -\frac{1}{2} & -\frac{1}{2} \\ 0 & \frac{\sqrt{3}}{2} & -\frac{\sqrt{3}}{2} \end{bmatrix}\begin{bmatrix} v_A \\ v_B \\ v_C \end{bmatrix} \tag{2}$$

$$\begin{bmatrix} v_d \\ v_q \end{bmatrix} = \begin{bmatrix} \cos(\omega_e t) & \sin(\omega_e t) \\ -\sin(\omega_e t) & \cos(\omega_e t) \end{bmatrix}\begin{bmatrix} v_\alpha \\ v_\beta \end{bmatrix} \tag{3}$$

where v_A, v_B and v_C are three – phase voltages in stationary frame, $v\alpha$ and $v\beta$ are two – phase voltages in stationary frame, v_d and v_q are voltages along d- and q- axis respectively on rotating reference frame and ω_e is electrical angular velocity.

In regards to an EV's PMSM, a stable working point between PMSM's electromagnetic torque and torques of resistance (or more commonly found as resistance forces, namely aerodynamic resistance, rolling resistance, uphill drive resistance, static and viscous friction). PMSM's electromagnetic torque is dependent on the flux linkage of permanent magnets in the rotor. Thus, having rotor's position determined in every single moment of time is essential for proper control of a PMSM. Electrical drives of operations, in which rotor's position or an accurate position of a detail are necessary, are controlled by utilizing vector control or also called field – oriented control (FOC). In essence FOC incorporates Clarke's and Park's transformations, applies a control method and further produces PWM signals by transforming the quantities back by inverse Clarke's and Park's transformations. However, in recent years, the method of SVPWM allows a space vector to be formed only by vectors in stationary reference frame. Thus, forward Park's, inverse Clarke's and inverse Park's transformations can be omitted. SVPWM is characterized with better DC voltage utilization (SPWM utilizes 3/4 while SVPWM utilizes √3/2 of DC bus voltage [2]), lower harmonic distortion, reduced switching losses when compared to sinusoidal PWM (SPWM). SVPWM, however, has the disadvantage that is more computationally intensive [6-8].

Considering the base voltage vectors from Table 1 and Fig. 2 the stator's space can be divided into sectors. A sector is defined as the space between the vectors formed by the six active combinations (hexagon from Fig. 2). The position of a space vector V_{ref} in time in each sector is determined by its magnitude M and angle (position) φ. The magnitude and angle are determined by two adjacent active vectors (V_1 to V_6) of each sector and the two null vectors (V_0 and V_7) [2, 5-7, 10, 12-14].

Having determined the voltages $v\alpha$ and $v\beta$ by applying Clarke's transformation, space vector's magnitude and angle can easily be calculated by (4) and (5) respectively [10, 14]. Forming a space vector V_{ref} in a specific sector and also its passing through to another sector can be determined by (6) and visualized by Fig. 3.

$$|V_{ref}| = \sqrt{(v_\alpha)^2 + (v_\beta)^2} \tag{4}$$

$$\varphi = \arctan\left(\frac{v_\beta}{v_\alpha}\right) \tag{5}$$

$$V_{ref} = V_x T1 + V_y T2 + V_{null} T0 \tag{6}$$

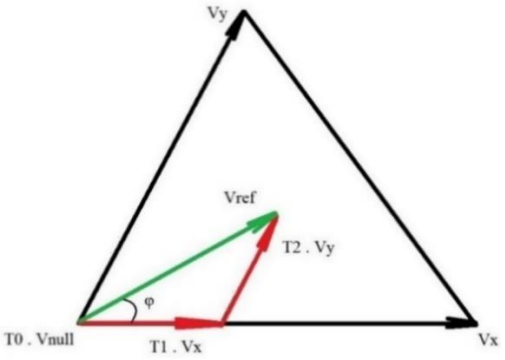

FIGURE 3. Formation of space vector V_{ref} in an arbitrary sector.

In order to accomplish the space vector rotation along the designated sectors, the switching time periods T_1, T_2 and T_0 must be calculated. From Fig. 3 it is observed that T_1 is the period in which V_x (the clockwise base vector of a given sector) is applied, T_2 is the period of applying V_y (the anti- clockwise base vector of a given sector) and T_0 is the time period for applying null vectors [10]. These time periods can be determined by (7) [5, 7, 8, 10, 13].

$$\begin{aligned} T1 &= Ta\sin(\frac{n}{3}\pi - \varphi) \\ T2 &= Ta\sin(\varphi - \frac{n-1}{3}\pi) \\ T0 &= T - \left(T1 + T2\right) \end{aligned} \tag{7}$$

where T is switching period, n is number of sector and a is a modulation index given by (8).

$$a = \frac{\sqrt{3}V_{ref}}{V_d} \tag{8}$$

where V_{ref} is modulated space vector voltage, V_d is the space vector voltage at hexagon's positions (complete DC voltage utilization).

TABLE 2. Reversing alternating sequence switching periods for each sector.

Sector number	Switching sequence of upper side switches	Switching sequence of lower side switches
1	$S_1 = T_1 + T_2 + (T_0/2)$ $S_3 = T_2 + (T_0/2)$ $S_5 = T_0/2$	$S_4 = T_0/2$ $S_6 = T_1 + (T_0/2)$ $S_2 = T_1 + T_2 + (T_0/2)$
2	$S_1 = T_1 + (T_0/2)$ $S_3 = T_1 + T_2 + (T_0/2)$ $S_5 = T_0/2$	$S_4 = T_2 + (T_0/2)$ $S_6 = T_0/2$ $S_2 = T_1 + T_2 + (T_0/2)$
3	$S_1 = T_0/2$ $S_3 = T_1 + T_2 + (T_0/2)$ $S_5 = T_2 + (T_0/2)$	$S_4 = T_1 + T_2 + (T_0/2)$ $S_6 = T_0/2$ $S_2 = T_1 + (T_0/2)$
4	$S_1 = T_0/2$ $S_3 = T_1 + (T_0/2)$ $S_5 = T_1 + T_2 + (T_0/2)$	$S_4 = T_1 + T_2 + (T_0/2)$ $S_6 = T_2 + (T_0/2)$ $S_2 = T_0/2$
5	$S_1 = T_2 + (T_0/2)$ $S_3 = T_0/2$ $S_5 = T_1 + T_2 + (T_0/2)$	$S_4 = T_1 + (T_0/2)$ $S_6 = T_1 + T_2 + (T_0/2)$ $S_2 = T_0/2$
6	$S_1 = T_1 + T_2 + (T_0/2)$ $S_3 = T_0/2$ $S_5 = T_1 + (T_0/2)$	$S_4 = T_0/2$ $S_6 = T_1 + T_2 + (T_0/2)$ $S_2 = T_2 + (T_0/2)$

There are multiple switching sequences, based on T_1, T_2 and T_0 durations for the upper side switch for each leg, that can be applied with SVPWM. Some of them utilize application of only one of the two null vectors, others utilize one of the null vectors in odd numbered sectors and the other in even numbered sectors and others - vice versa. Most commonly implemented method of SVPWM is, however, the reversing alternating sequence [5, 8, 10, 13, 14] (can be

also found as 7 – segment sequence in [7]). In the reversing alternating sequence both null vectors V_0 and V_7 are utilized in an alternating way. Implementing the null vectors in such a way allows for a control method with reduced number of switching and thus reduced switching losses [10]. That is to say that for example let a switching period T occurs in *sector 1*, formed by V_1, V_3 and V_0 by their respective durations T_1, T_2 and T_0, and if this particular switching sequence has to be run backwards, it doesn't have to begin with V_1 again. Following the next switching period will incorporate V_7 and so on.

The reversing alternating sequence for each switch in inverter's legs and for each sector is shown in Table 2. The periods for lower side switches are considered as complementary to respective upper side one.

MODELLING OF SPACE VECTOR MODULATION

Modelling of SVPWM is done in MATLAB/ Simulink environment. The model presented in this paper fulfills the purpose of introducing SVPWM as one of the most utilized and advantageous control algorithm purely on a simulation level. It presents a simple implementation of the control method applied to the equivalent circuit of an EV's powertrain system. Furthermore, it allows for simulation of the motor operating as a generator whenever the vehicle is regenerative braking. Further complications and more accurate models with experimental stand will be done in future works. The model is shown on Fig. 4 and consists of a PMSM, a three – phase MOSFET power converter, a measurements subsystem with which simulation results are visualized and an SVPWM subsystem.

PMSM is modelled with sinusoidal back electro motive force and as a 4 poled non – salient pole machine (surface mount PMSM). Surface mount PMSM's inductances across d and q axes are equal ($L_d = L_q$). The simulation block of the motor allows to be controlled by a mechanical input or by an angular velocity input. In this model it is chosen to be controlled by a mechanical torque input.

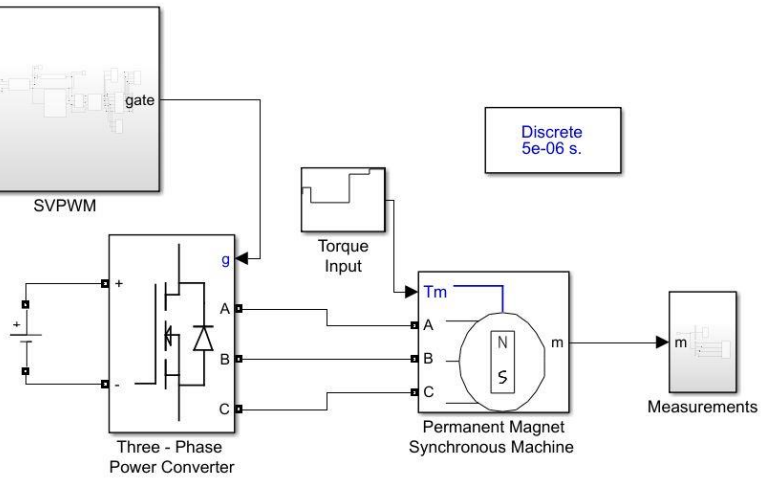

FIGURE 4. Proposed Simulink model.

The modelling approach, taken in SVPWM subsystem, consists of performing Clarke's transformation, formation of sectors, computation of switching periods T_1, T_2 and T_0, and further utilizing them to produce PWM signals by comparison to a sawtooth wave signal. Details for each part of SVPWM subsystem are presented further below.

Clarke's transformation is simulated by implementing (2) as shown on Fig. 5. Obtained alpha and beta components are shown on Fig. 6. Formed voltages v_α and v_β are used to form space vector V_{ref} and its angle φ accordingly to (4) and (5), and their time relation is shown on Fig. 7.

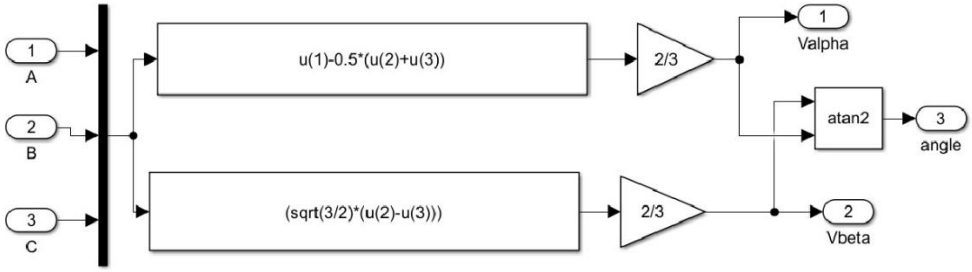

FIGURE 5. Implementation of Clarke's transformation

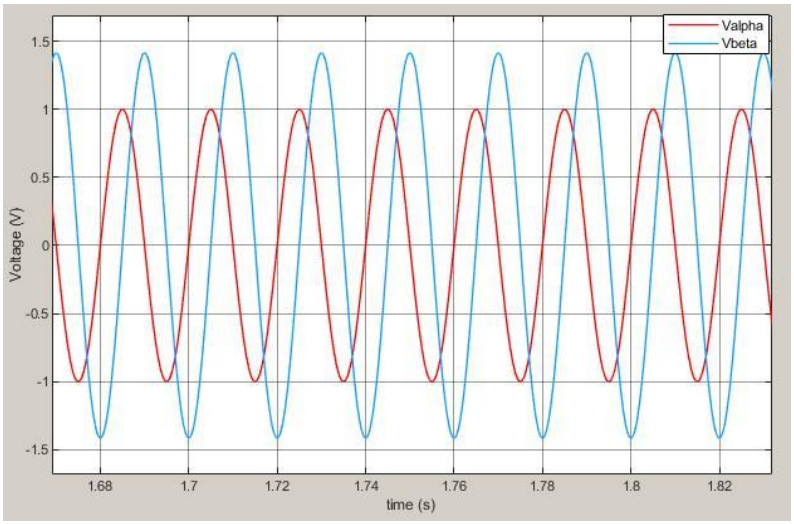

FIGURE 6. Alpha and beta components

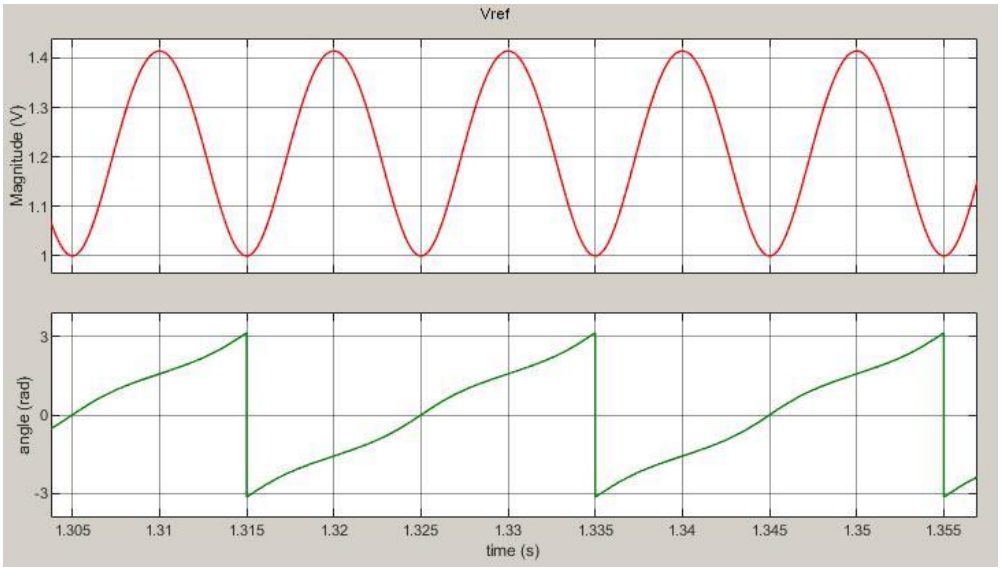

FIGURE 7. Magnitude and angle of V_{ref} in time.

The obtained angle φ is further used in determination of sectors in sector formation's subsystem. Sector's subsystem is shown on Fig. 8 and resulting space vector's passing through each sector is given on Fig. 9. It can be seen that space vector passes through each of the six sectors successfully in time.

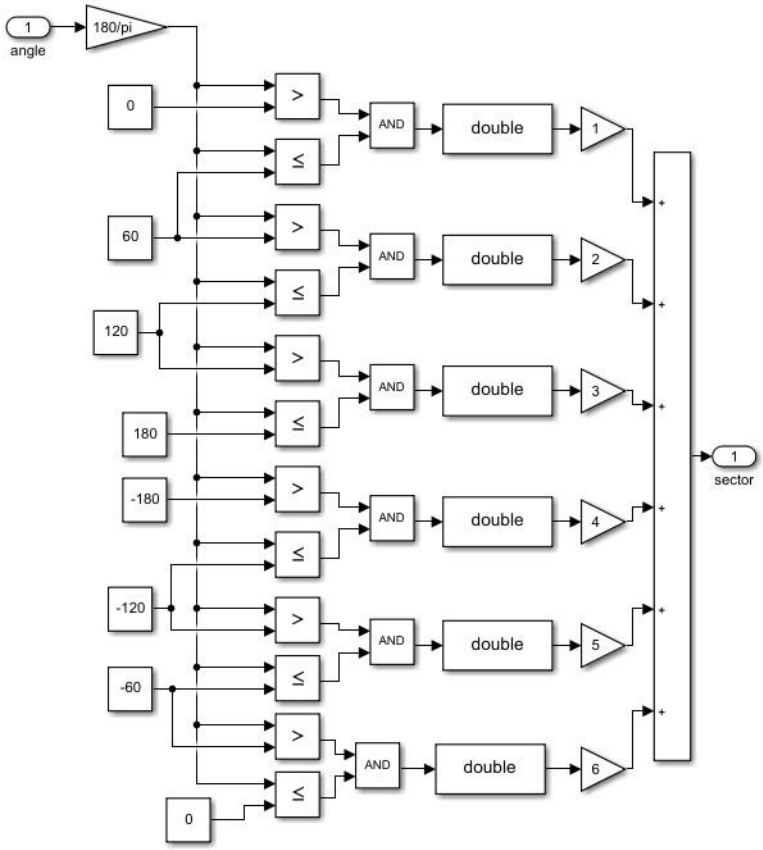

FIGURE 8. Sector's formation subsystem

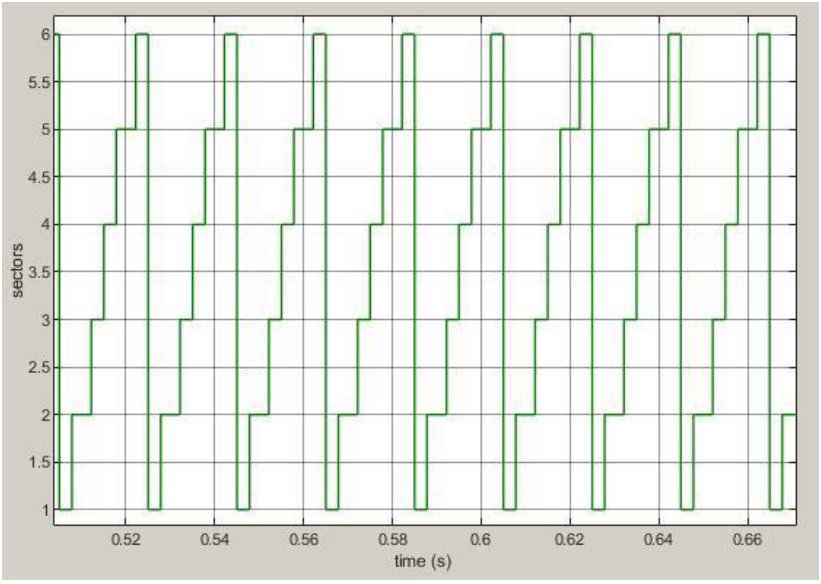

FIGURE 9. Space vector passing through sectors in time

After defining sectors and passing the space vector through each of them, the durations T_1, T_2 and T_0 are calculated. Calculations of T_1, T_2 and T_0 for reversing alternating sequence follows (6), (7) and (8), and are implemented as shown on Fig. 10. The switching period's T value is considered 20 ms, as it corresponds to the period of sine waves with frequency of 50 Hz. Following that, T_1, T_2 and T_0 are applied on switch blocks to produce reversing alternating sequence accordingly to Table 2.

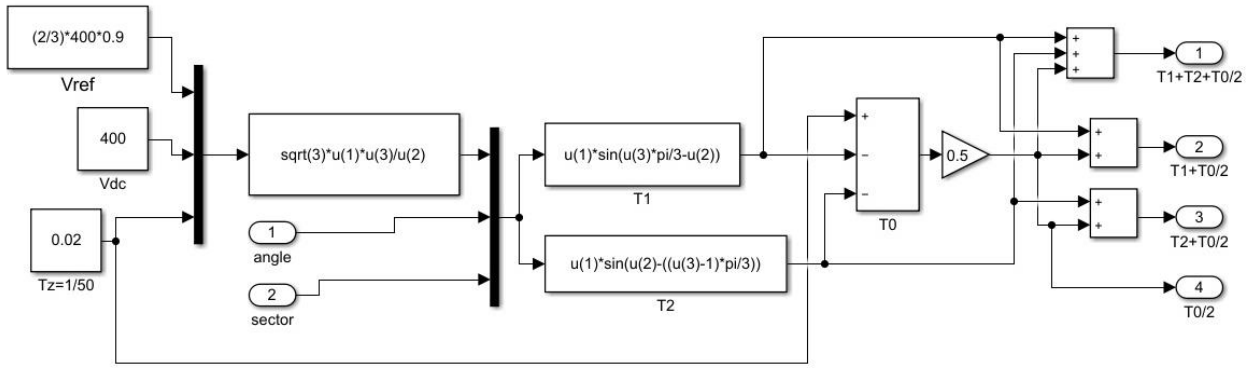

FIGURE 10. Implementation of calculations of time periods T_1, T_2 and T_0.

Results for upper side switches of the inverter, termed namely 1, 3 and 5 are shown on Fig. 11. Analogously, respective results for each power switch is further compared to a sawtooth wave signal with 20 kHz frequency to produce PWM duty cycles. They are further applied to the inverter's gate port termed *g* as shown on Fig. 4.

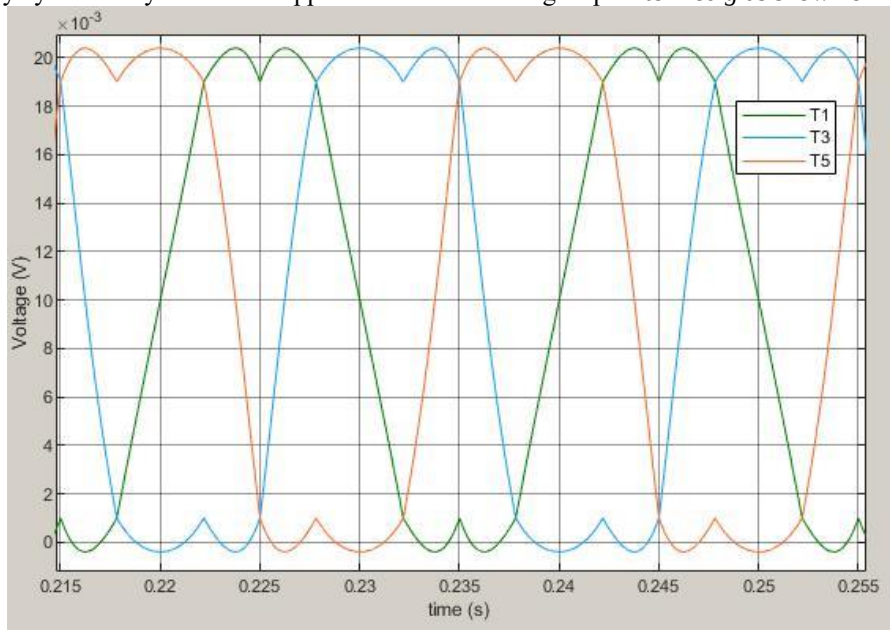

FIGURE 11. Reversing alternating sequence for upper side switches.

The overall model simulation runs for 25 seconds. There are periods with different situations that are considered. Period from 3rd to 10th second and the period from 18th to 25th second are considered as braking periods and are utilized to examine the simulation with possibilities of regenerative braking. In regenerative braking the wheels are driving the machine (generator operation) as their mechanical angular velocity is higher than the electrical angular velocity of the electrical machine. This causes the rotation to be kept in the same direction and only the torque to change its sign (second quadrant of the mechanical characteristic of the motor in forward direction).

The remaining periods are considered for forward propellment of the EV. The mechanical input torque T_m is shown on Fig. 12. It is simulated with amplitude between 1 and 3.5 Nm for periods of forward motion and an amplitude between 1 and 5 Nm for braking periods. The direction of propelling (PMSM operating as a motor) is taken as positive, hence braking is modelled with negative torque values.

Obtained results are purely on simulation level and are utilized to show that the expected nature of electrical and mechanical quantities in steady state and transients is achievable even with simpler models.

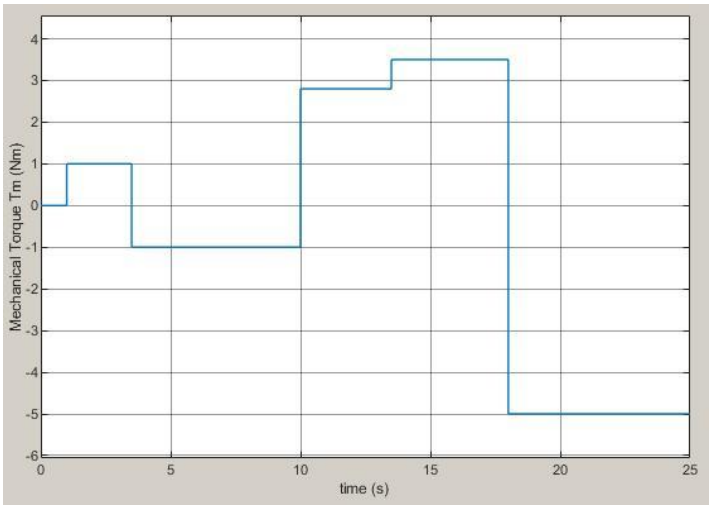

FIGURE 12. Mechanical torque input *Tm*

PMSM's electromagnetic torque, T_e, is presented on Fig. 13. It can be seen that during steady state T_e corresponds to T_m accordingly. Negative values of T_e exhibit operation of the motor as a generator as expected. However, on the figure during changes in T_m's values there are present transients with significant amplitudes. These high amplitudes are caused by simplicity of the model and lack of feedback loop.

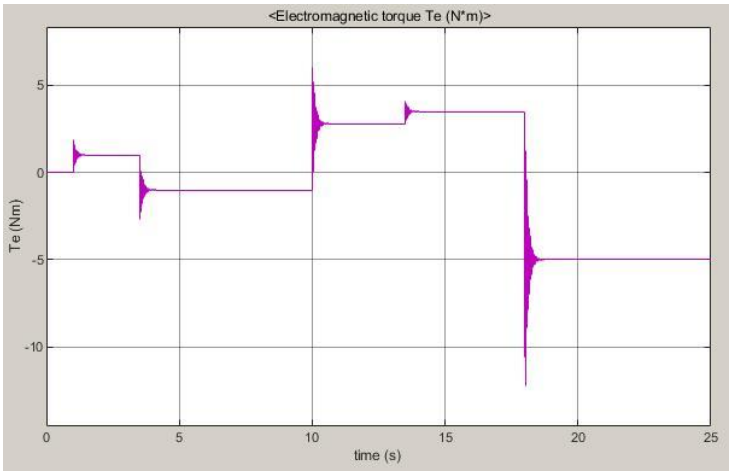

FIGURE 13. PMSM's electromagnetic torque *Te*.

Obtained results of PMSM's three – phase stator currents are shown on Fig. 14. It can be seen that they exhibit sinusoidal waveforms, which are more distinguished with higher torque values. There are also present noticeable current transients, corresponding to torque's transients. This can be attributed to the modelled values of PMSM's viscous damping coefficient and moment of inertia.

By these obtained waveforms it seems that with longer simulation and higher values of implemented electrical and mechanical quantities, even such a simple model may produce results of three – phase currents with low harmonics.

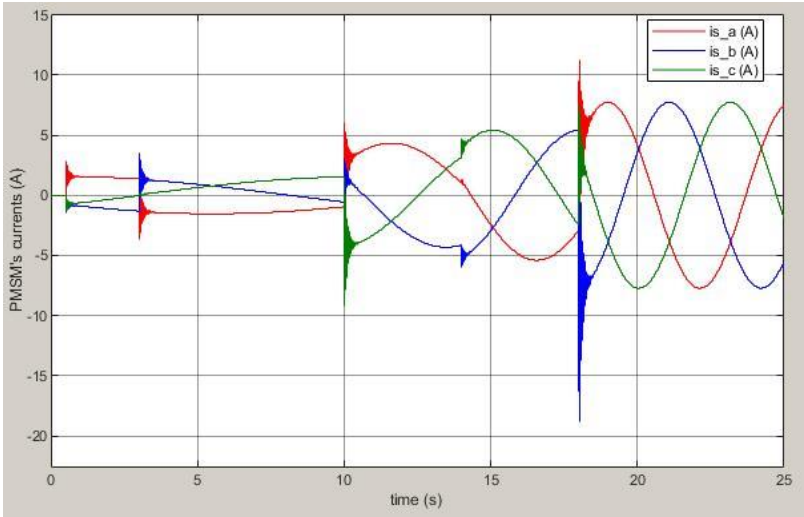

FIGURE 14. PMSM's three – phase stator currents.

CONCLUSION

A discussion about modelling of SVPWM for EV application is presented in this paper. SVPWM is one of widely applied algorithms in FOC. The approach of modelling consists of implementation of Clarke's transformation, formation of a space vector and its rotation along sectors in time, determination of time periods T_1, T_2 and T_0 for reversing alternating switching sequence, which are further utilized in PWM to produce duty cycles for power switches. The control algorithm simulated in such way is further utilized to control electrical quantities of a PMSM with considerations of possibilities of regenerative braking.

Based on simulation results it is observed that space vector is passing through the designated sectors successfully. The output voltages of inverter's switches exhibit the expected waveforms (sinusoidal with two maximums) of reversing alternating sequence SVPWM. Furthermore, PMSM's electromagnetic torque corresponds to the mechanical torque input during steady state. Motor's currents also exhibit sinusoidal waveforms, although having the same fluctuations during transients as electromagnetic torque. This can be attributed to PMSM's simulated viscous damping and inertia. Overall it can be concluded that SVPWM control in an open loop nature circuit has been achieved with satisfactory results. Additional work in the direction of making the model more accurate and more complex is required. It is likely to be done in further works.

ACKNOWLEDGMENT

The authors would like to thank the Research and Development Sector at the Technical University of Sofia for the financial support.

REFERENCES

1. K. Bimal, *Modern Power Electronics and AC Drives* (Prentice-Hall, 2001).
2. M. Antchev, *Power Electronic Devices. Textbook for Students of Technical University of Sofia* (Technical University of Sofia, 2008), (In Bulgarian).
3. A. Berzov, J. Viola and J. Restrepo, "Voltage space vector's computation for current control in three phase converters", Revista Facultad de Ingeniería Universidad de Antioquia **64**, pp. 45–56 (2012).
4. Texas Instruments, Space-Vector PWM with TMS320C24x/F24x Using Hardware and Software Determined Switching Patterns, March 1999, Literature Number SPRA524.
5. A. Iqbal, A. Lamine, I. Ashraf and Mohibullah, "Matlab/Simulink Model of Space Vector PWM for Three-Phase Voltage Source Inverter", *Proceedings of the 41st International Universities Power Engineering Conference*, IEEE, pp. 1096–1100 (2006).

6. Y. Ma, L. Fan and Z. Miao, “Realizing space vector modulation in MATLAB/Simulink and PSCAD”, *2013 North American Power Symposium (NAPS)*, IEEE, pp. 1–6 (2013).
7. P. Tripura, Y. Babu and Y. R. Tagore, “Space vector pulse width modulation schemes for two-level voltage source inverter”, ACEEE Int. J. on Control System and Instrumentation **2**(3), pp. 34–38 (2011).
8. F. R. Yasein and R. A. Mahmood, “Design new control system for brushless DC motor using SVPWM” International Journal of Applied Engineering Research **13**(1), pp. 582–589 (2018).
9. W.-F. Zhang and Y.-H. Yu, “Comparison of three SVPWM strategies”, Journal of Electronic Science and Technology of China **5**, pp. 283–287 (2007).
10. Texas Instruments, Dave Wilson, “Teaching Old Motors New Tricks” seminar videos, February 2014.
11. K. T. Chau, *Electric Vehicle Machines and Drives: Design, Analysis and Application* (John Wiley & Sons, Singapore Pte. Ltd., 2015).
12. T. Liu, Y. Tan, G. Wu and S. Wang, “Simulation of PMSM vector control system based on Matlab/Simulink”, *2009 Int. Conf. on Measuring Technology and Mechatronics Automation*, IEEE, pp. 343–346 (2009).
13. A. Saritha, T. Abhiram, Dr. K. Sumanth, “Space vector pulse width modulation for two level inverter”, International Journal of Professional Engineering Studies (IJPRES) **6**(3), pp. 8–14 (2016).
14. M. Kubeitari, A. Alhusayn and M. Alnahar, “Space vector PWM simulation for three phase DC/AC inverter”, International Journal of Electrical and Computer Engineering **6**(12), Version 5205, pp. 1402–1407 (2012).